Microchimica Acta (2021) 188: 208
https://doi.org/10.1007/s00604-021-04869-z

ORIGINAL PAPER

An electrochemical sensor for voltammetric detection of ciprofloxacin using a glassy carbon electrode modified with activated carbon, gold nanoparticles and supramolecular solvent

Netsirin Gissawong[1] · Supalax Srijaranai[1] · Suthasinee Boonchiangma[1] · Pikaned Uppachai[2] · Kompichit Seehamart[2] · Sakwiboon Jantrasee[2] · Eric Moore[3] · Siriboon Mukdasai[1]

Received: 10 March 2021 / Accepted: 17 May 2021 / Published online: 28 May 2021

Abstract

A highly sensitive and novel electrochemical sensor for ciprofloxacin (CIP) has been developed using gold nanoparticles deposited with waste coffee ground activated carbon on glassy carbon electrode (AuNPs/AC/GCE) and combined with supramolecular solvent (SUPRAS). The fabricated AuNPs/AC/GCE displayed good electrocatalytic activity for AuNPs. The addition of SUPRAS, prepared from cationic surfactants namely didodecyldimethylammonium bromide (DDAB) and dodecyltrimethylammonium bromide (DTAB), increased the electrochemical response of AuNPs. The detection of CIP was based on the decrease of the cathodic current of AuNPs. The electrochemical behavior of the modified electrode was investigated using cyclic voltammetry, differential pulse voltammetry and electrochemical impedance spectroscopy. Under optimum conditions, the calibration plot of CIP exhibited a linear response in the range 0.5–25 nM with a detection limit of 0.20 nM. The fabricated electrochemical sensor was successfully applied to determine CIP in milk samples with achieved recoveries of 78.6–110.2% and relative standard deviations of <8.4%. The developed method was also applied to the analysis of pharmaceutical formulation and the results were compared with high-performance liquid chromatography.

Keywords Gold nanoparticles · Activated carbon · Supramolecular solvent · Ciprofloxacin · Electrochemical sensor

Introduction

Ciprofloxacin (CIP) is an antibiotic in the fluoroquinolones (FQs) groups. They have been used in livestock and humans for the treatment of various infectious diseases such as respiratory, urinary tract, gastroenteritis, ocular and skin infections [1–3]. CIP can be residual in animal-derived foodstuffs and results in various undesirable effects to the consumers including hypersensitive, immunotoxicity, carcinogenicity, genotoxicity and endocrine disruptors [4]. The European Union (EU) established the maximum residue limit (MRL) of CIP in combination with its active metabolite, enrofloxacin, at 100 μg kg^{-1} for animal products [5, 6]. Based on the low MRL of CIP, various sensitive and effective methods have been developed for CIP determination including UV–Vis spectrophotometry [7, 8], fluorescence spectroscopy [9, 10] and high-performance liquid chromatography [11, 12].

Another popular method utilizes electrochemical sensors. These are simple, cost-effective, fast response time and are relatively user friendly [13, 14]. Many electrodes have been successfully used for CIP detection. These include glassy carbon electrode (GCE) [15, 16], graphite electrode (GE) [17], boron-doped diamond printed electrode (BDDP) [18], and screen-printed electrode (SPE) [19]. As the electrode is the critical aspect for the method performance, modification of the electrode surface has attracted increasing attention [20].

✉ Siriboon Mukdasai
sirimuk@kku.ac.th

[1] Materials Chemistry Research Center, Department of Chemistry and Center of Excellence for Innovation in Chemistry, Faculty of Science, Khon Kaen University, Khon Kaen 40002, Thailand

[2] Department of Applied Physics, Faculty of Engineering, Rajamangala University of Technology Isan, Khon Kaen Campus, Khon Kaen 40000, Thailand

[3] School of Chemistry and Tyndall National Institute, University College Cork, Cork, Ireland

Various carbon nanomaterials have been extensively applied to modify the surface of electrode for the CIP detection such as carbon nanotubes (CNTs) [21, 22] and graphene oxide (GO) [15, 16]. They have good properties for electroanalysis including high conductivity, large surface-to-volume ratio and high electron mobility at room temperature [14]. Activated carbon (AC) is one such carbon material and it has been recognized as an efficient material for various applications. AC can be prepared from bio-wastes which makes the preparation process simple, eco-friendly and cost-effective. It has been widely used in supercapacitor applications because of its excellent electrical conductivity, high surface area and thermal stability [23–25]. Recently, metal nanoparticles such as silver nanoparticles (AgNPs) and gold nanoparticles (AuNPs) have been increasingly employed in biosensor, chemisensor and electrocatalyst fields. These types of nanoparticles have magnetic, electronic, optical and catalytic properties which facilitate electron transfer of redox reactions [26]. There are many reports using carbon nanomaterials combined with metal nanoparticles to enhance the electrochemical response for the detection of FQs. Examples of these include gold–palladium nanoparticles/GO [27], AuNPs/GO/MWCNT [28], AgNPs/carbon black [29], AuNPs/GO [30] and CuNPs/graphene [31].

Other promising substances used to improve electrochemical sensitivity are surfactants. They not only increase reaction rates and the kinetics of electron transfer reactions, but also control the solubilization of organic compounds for electroanalysis in water [32]. Various surfactants have been employed such as sodium dodecyl sulfate (SDS) for detection of nicotine [33, 34], tetrabutylammonium bromide (TBABr) for L-tryptophan detection [20], and cetyltrimethylammonium bromide (CTAB) for the determination of gatifloxacin and pefloxacin [31]. More recent, supramolecular solvents (SUPRASs) have been of extreme interest due to their green characteristics, i.e., non-volatile and non-flammable. SUPRASs are nanostructured liquids obtained from self-assembly of amphiphiles and include surfactants under coacervation conditions such as temperature, pH or electrolyte [35]. One of the attractive properties of SUPRASs is tunability of polarity; thus, many interactions with target compounds can be achieved such as hydrogen bonding, π–π, π–cation, hydrophobic and electrostatic interactions [36]. To the best of our knowledge, the application of SUPRAS in electrochemical sensors has been rarely reported, making it a challenge to investigate for enhancement of the electrochemical sensitivity. Our previous research presented supramolecular electrochemical sensor for the detection of dopamine using AuNPs/GO/GCE. Mixed surfactants containing cationic surfactant (TBABr) and anionic surfactant (SDS) were used to increase the interface property between the surface of electrode and the target analyte. This sensor has excellent electrocatalytic activity toward the dopamine oxidation and successfully applied for human serum [37].

Herein, this is the first report for the detection of ciprofloxacin (CIP) using glassy carbon electrode (GCE) modified with gold nanoparticles deposited activated carbon (AuNPs/AC) combined with SUPRAS. In this study, AC was synthesized from waste coffee grounds, while the SUPRAS were prepared from cationic surfactants namely didodecyldimethylammonium bromide (DDAB) and dodecyltrimethylammonium bromide (DTAB) in the presence of NaCl as a coacervating agent. The electrochemical sensors of CIP detection are mostly based on the increasing of its peak current [15–19]. This work proposed an indirect sensor for CIP determination by detection the decreasing of AuNPs cathodic current in the presence of CIP. The modification of GCE with AC, AuNPs and SUPRAS provided the electrochemical sensitivity and selectivity for CIP detection. All experimental parameters including the modification of electrode surfaces and electrochemical behavior of CIP were thoroughly investigated. The proposed electrochemical sensor was then successfully applied to determine CIP in milk and pharmaceutical samples.

Experimental

Materials and chemicals

All of chemicals were analytical reagent grade and obtained from various suppliers including ciprofloxacin (CIP), enrofloxacin (ENR), norfloxacin (NOR), ofloxacin (OFL), tetracycline hydrochloride (TC), oxytetracycline hydrochloride (OTC) and amoxicillin (AMX) from Sigma–Aldrich (USA and China). Didodecyldimethylammonium bromide (DDAB) and dodecyltrimethylammonium bromide (DTAB) were acquired from Fluka (Denmark) and Sigma–Aldrich (India), respectively. Gold(III) chloride trihydrate ($HAuCl_4$ $3H_2O$) and potassium hexacyanoferrate(III) ($K_3Fe(CN)_6$) were obtained from Sigma–Aldrich (USA and Spain). Sodium chloride (NaCl), potassium chloride (KCl), potassium hydroxide (KOH) and sodium dihydrogen phosphate dihydrate (NaH_2PO_4 $2H_2O$) from Ajax finechem (New Zealand), sodium hydroxide (NaOH) from Carlo Erba (France) and 95–97% sulfuric acid (H_2SO_4) from Merck (Germany) were used. Disodium hydrogen phosphate (Na_2HPO_4), 85% phosphoric acid (H_3PO_4), 85% formic acid (HCOOH) and N,N–dimethylformamide (DMF) were obtained from QRëC (New Zealand). HPLC–grade methanol (MeOH) and acetonitrile (ACN) were acquired from LiChrosolv (China). Deionized water produced from RiOs™ Type I Simplicity 185 (Millipore water, USA) with a specific resistivity of 18.2 MΩ cm, was used throughout.

The stock solution (1000 mg L^{-1}) and the working standard solution of CIP were prepared by dissolving an appropriate amount in 0.1 M NaOH and daily stepwise dilution of the stock solution with deionized water, respectively. The stock

solution of DTAB (50 mM) and DDAB (25 mM) was prepared in deionized water. Phosphate buffers with various pH were prepared by mixing 0.1 M Na_2HPO_4 and 0.1 M NaH_2PO_4 $2H_2O$ at different ratios, and adjusted by adding 0.1 M H_3PO_4 or 0.1 M NaOH.

Instrumentation

All electrochemical experiments including cyclic voltammetry (CV), differential pulse voltammetry (DPV) and electrochemical impedance spectroscopy (EIS) were performed on an AutoLab PGSTAT302N (Utrecht, Switzerland) at room temperature. A three-electrode system was used including 5-mm glassy carbon electrode (GCE; CorrTest, Hebei, China) modified with activated carbon (AC), prepared from waste coffee grounds, and then deposited AuNPs (AuNPs/AC/GCE) was used as working electrodes, a platinum wire as counter electrode (CorrTest, Hebei, China), and Ag/AgCl (3 M KCl) as reference electrode (CorrTest, Hebei, China). The surface morphology and composition of the modified electrodes were conducted by focused ion beam scanning electron microscopy (FIBSEM) and energy-dispersive X-ray spectroscopy (EDS) analysis (Helios NanoLab G3 CX, FEI, USA). X-ray photoelectron spectroscopy (XPS; AXIS Ultra DLD, UK) was employed to analyze the structure of AC. Dynamic light scattering (DLS) (Zetasizer Nano ZS, UK) was used to determine zeta potential of SUPRAS and CIP–SUPRAS. Moreover, high-performance liquid chromatography (HPLC) was used to detect CIP in real samples for comparison with the fabricated electrochemical sensor. The HPLC system composed of an Agilent 1220 LC system VL, a binary pump, a manual injector with a sample loop of 20 μL, and an Agilent 1260 Infinity II multiple wavelength detector (MWD). Data acquirement and processing were accomplished using OpenLAB CDS Chemstation software. The chromatographic separation of CIP was completed within 4 min using an ACE Excel5 C18–AR (150 mm × 4.6 mm i.d., 5.0 mm) column (Advanced Chromatography Technologies) with isocratic elution using a mixture of ACN and 0.1% HCOOH at ratio of 20/80 (*v*/v), at a flow rate of 1.0 mL min^{-1} and detection at 280 nm.

Preparation of the AuNPs/AC/GCE

Activated carbon (AC) was synthesized from waste coffee grounds using protocols from previous research with some modifications to the procedure [38]. The waste coffee grounds were prepared from coffee beans and filled in a coffee machine. The waste coffee powder was cleaned by 0.5 M KOH to remove the interferences and dried in an oven for 2 h at 80 °C. The waste coffee ground precursor was then obtained and placed in the hydrothermal autoclave with 60 mL of 1 M KOH to produce the porous carbons. The autoclave was heated at temperature 150 °C by the in-house high power microwave furnace for 30 min and the homogeneous AC product was obtained. The AC (5 mg) was dissolved in DMF (1 mL) and the homogenous suspension was acquired after sonication for 30 min. Glassy carbon electrode (GCE) was polished using 0.3 and 0.05 μm alumina slurry and cleaned ultrasonically in methanol first for 10 min and then in water for another 10 min. After that, 3 μL of AC dispersion (Fig. S1, see Supplementary) was dropped on the top of the polished GCE, allowing the solvent to evaporate at room temperature. The AC/GCE electrode was thus obtained.

To prepare AuNPs/AC/GCE, the AC/GCE electrode was immersed in 0.05 M H_2SO_4 containing 5.0 mM $HAuCl_4$ $3H_2O$. The electrodeposition of AuNPs was conducted for 30 s at −1.0 V (Fig. S2, Supplementary). Finally, the AuNPs/AC/GCE electrode was cleaned by applying a potential scan of −1.0 V to +1.2 V with a scan rate of 100 mV/s in phosphate buffer (pH 6.0) until a steady voltammogram was achieved.

Preparation of cationic SUPRAS

The cationic SUPRAS was prepared according to our previous report [39]. Briefly, 1 mL of 25 mM DDAB and 1 mL of 50 mM DTAB were placed in a centrifuge tube and adjusted to 10 mL with deionized water. The cloudy solution was formed after adding NaCl (1.5 g) and completely dissolved NaCl solution by manual shaking. It was then vortexed for 5 s and centrifuged at 3000 rpm for 1 min. Finally, the SUPRAS was found in the upper phase, collected by a syringe and kept in a vial until use.

Milk sample preparation

Milk samples including raw milk, UHT milk and 0% fat milk were purchased from a supermarket in Khon Kaen, Thailand. Two milliliter of milk was deproteinized and defatted using 100 μL of SUPRAS. After that, the solution was mixed by a vortex stirrer at 1800 rpm for 1 min and then centrifuged at 6000 rpm for 5 min. The supernatant was filtered through a 0.45-μm membrane filter (VertiClean™ NYLON) and then mixed with phosphate buffer (pH 10.0) at the ratio of 1/4 (v/v) before the analysis by the proposed electrochemical sensor.

Tablet sample preparation

Two 500-mg CIP tablet samples of Siam Cifloxin® and Farmaline Ciproxyl® were used. They are white tablet and ellipse shape which their masses are 0.7796 ± 0.0081 and 0.8278 ± 0.0084 g per tablet, respectively. The tablet was ground and weighted 50 mg. After that, it was dissolved with deionized water until complete dissolution, except its coverlayer. The obtained solution was filtered through a Whatman® (No. 42) filter paper and then it was adjusted to an appropriate volume with deionized water before the analysis by the proposed electrochemical sensor.

Electrochemical analysis of ciprofloxacin

A 5mL- standard CIP or sample solution in phosphate buffer (pH 10.0) was detected by differential pulse voltammetry (DPV). The prepared cationic SUPRAS (100 μL; Fig. S3, Supplementary) was added into the solution and then stirred for 20 s prior to electrochemical analysis using the AuNPs/AC/GCE. DPV measurements were performed from +1.2 to +0.2 V with the parameters of deposition potential: 0.6 V, deposition time: 10 s, pulse amplitude: 0.05 V, pulse time: 0.05 s and step potential: −0.005 V.

Results and discussion

Choice of materials

Ideal materials for good electrochemical performance are those having high surface area, excellent electrical conductivity, and chemical stability [20]. To obtain high sensitive and selective sensor, three materials including AC, AuNPs and SUPRAS were chosen for modification of GCE. AC synthesized from waste coffee grounds was selected because of its high surface area and good electrical conductivity. Similar to other metal oxides and metal nanoparticles, AuNPs was employed as its high capability to facilitate the electron transfer [40]. In addition, SUPRAS was used to increase sensitivity of the sensor from the enhancement of electron transfer and the enrichment of CIP toward the electrode surface. The schematic illustration of the AuNPs/AC/GCE and SUPRAS–AuNPs/AC/GCE sensors for CIP detection is depicted in Fig. 1.

Characterization of the modified electrode

The chemical composition of synthesized AC was studied by X-ray photoelectron spectroscopy (XPS) analysis as the result shown in Fig. 2. The XPS survey spectrum (Fig. 2A) indicated that the synthesized AC composed of carbon and oxygen atoms at 285.0 and 532.0 eV, respectively. The high-resolution C1s spectra (Fig. 2B) revealed that the C1s peak at binding energies of 285.0, 286.1, 286.9, and 288.0 eV corresponds to C=C and C–C, C–O, C=O and O–C=O, respectively [41, 42]. It was confirmed that AC has sp^2-hybridized carbon atoms; thus, good electrical conductivity is expected [43].

The surface morphology and composition of AC/GCE, AuNPs/AC/GCE and SUPRAS–AuNPs/AC/GCE were characterized by scanning electron microscopy (SEM) and energy-dispersive X-ray spectroscopy (EDS). Figure 2C illustrates the surface morphology of the AC which shows the irregular shapes with the diameter of 2 ± 0.22 μm ($n = 20$). After the deposition of AuNPs, the roughly spherical shape of AuNPs (particle size of 70 ± 6.68 nm; $n = 20$) was observed as can be seen as light dots in Fig. 2D, confirmed that the AuNPs was deposited on AC. Moreover, EDS and elemental mapping analysis (Figs. S4 and S5) showed that the synthesized AC consisted of only carbon atoms, while AuNPs/AC/GCE not only found carbon (C) atoms but also gold (Au) atoms indicating the existence of AuNPs. For SUPRAS–AuNPs/AC/GCE, Fig. 2E displays the well dispersion of AuNPs on AC

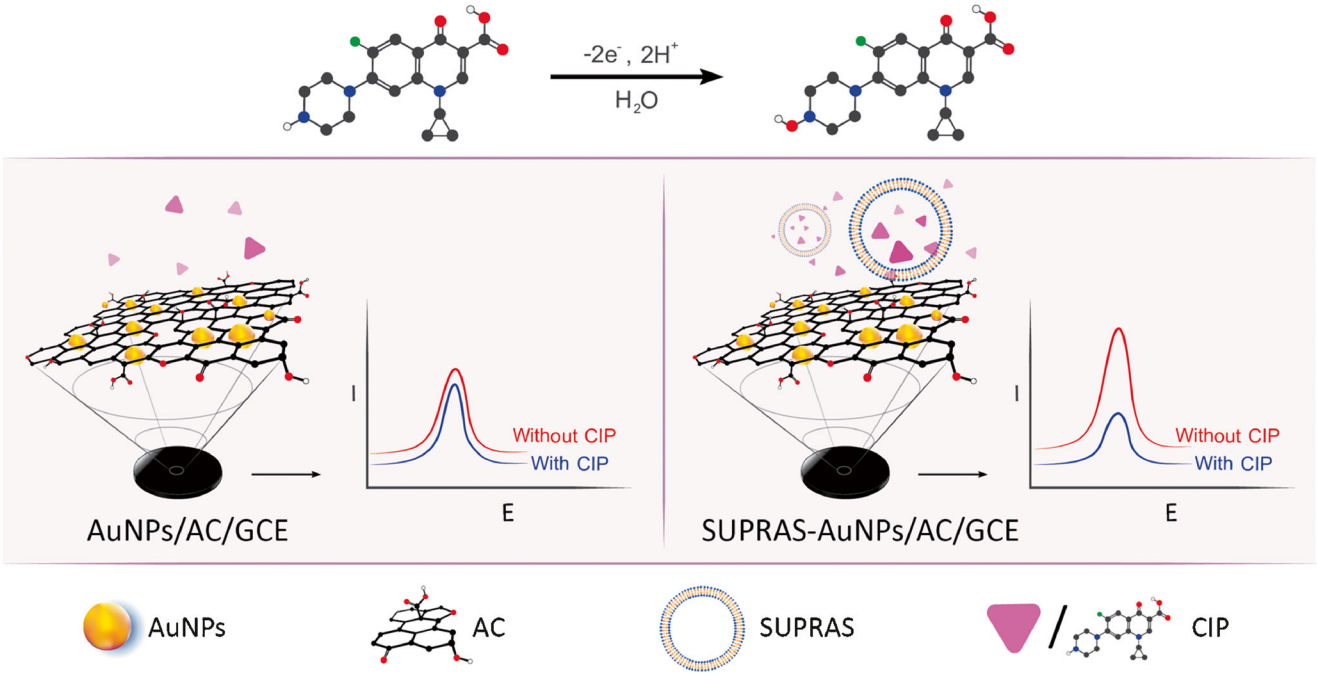

Fig. 1 The schematic diagram of the AuNPs/AC/GCE and SUPRAS–AuNPs/AC/GCE sensors for the detection of CIP

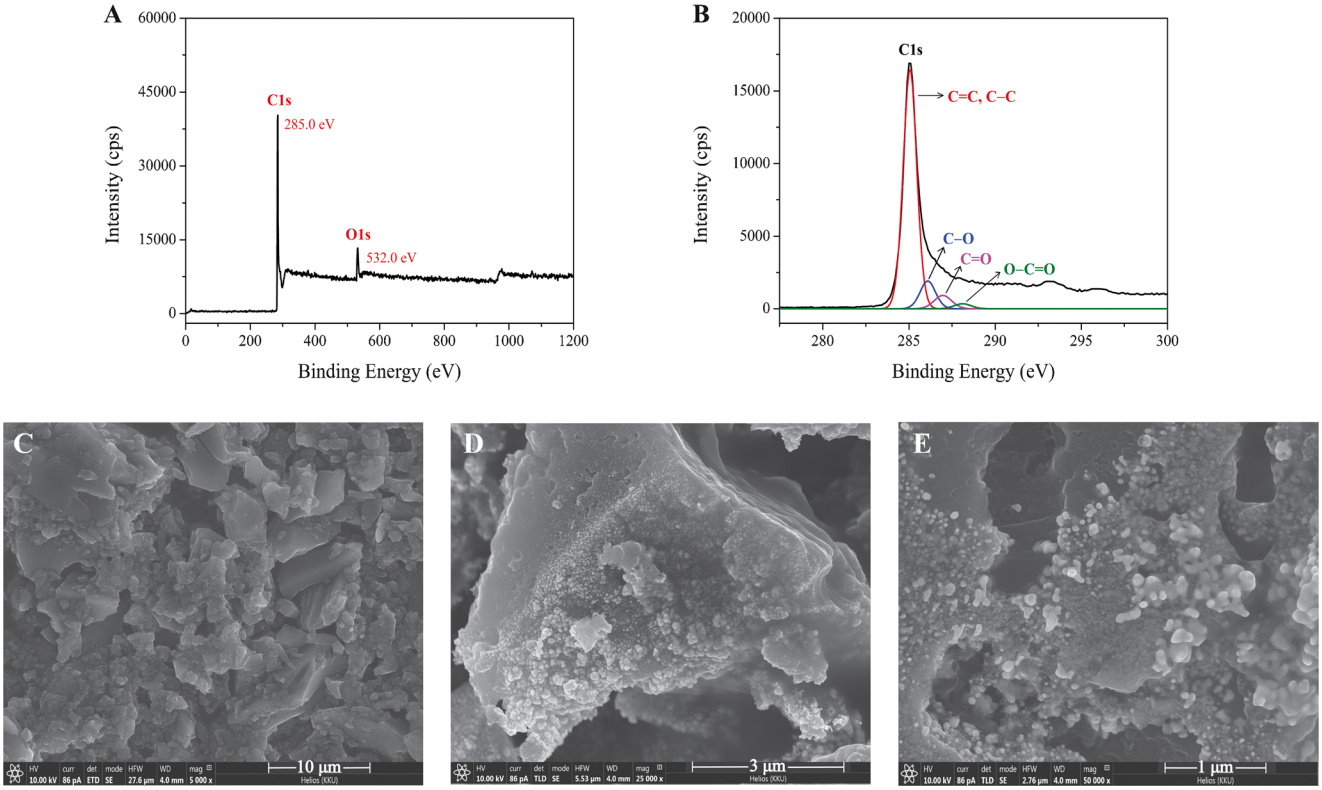

Fig. 2 (**A**) XPS survey spectrum of AC, (**B**) XPS high-resolution spectra of the C1S region of AC, SEM images of (**C**) AC, (**D**) AuNPs/AC and (**E**) SUPRAS–AuNPs/AC

in the presence of SUPRAS which covered AuNPs resulted the larger particle size of 125 ± 7.33 nm (n = 20). The EDS and elemental mapping results (Fig. S6) revealed the existence of bromine (Br) and chlorine (Cl) atoms in SUPRAS which these elements are well dispersion; hence, it can be confirmed the complete fabrication of the proposed electrode.

The electrochemical performance of the modified electrode was studied by cyclic voltammetry (CV) using 5 mM $[Fe(CN)_6]^{3-/4-}$ containing 0.1 M KCl. As the results displayed in Fig. 3A, the response current of $[Fe(CN)_6]^{3-/4-}$ at bare GCE was the lowest value with the peak separation (ΔE) of 0.40 V obtained from anodic peak at 0.56 V and cathodic peak at −0.16 V because of small surface area (0.0468 cm^2) and weak conductivity. After the modification with either AuNPs or AC (AuNPs/GCE and AC/GCE), the peak currents were clearly increased and the peak potentials were shifted to negative value of anodic peaks at 0.28 V and positive value of cathodic peaks at 0.19 and 0.20 V, provided ΔE of 0.09 and 0.08 V for AuNPs/GCE and AC/GCE, respectively. It revealed that AuNPs and AC can increase the surface area and conductivity, thus accelerate electron transfer between $[Fe(CN)_6]^{3-/4-}$ and electrode [28, 44]. Consequently, when the two materials were combined (i.e., AuNPs/AC/GCE), the highest electrochemical response was achieved which arisen from a synergistic effect of AuNPs and AC. The anodic peak of 0.26 V and cathodic peak of 0.19 V with ΔE of 0.07 V were obtained on AuNPs/AC/GCE, indicated that electron transfer was facilitated. According to the Randles–Sevcik equation [45], the electroactive surface area was also calculated by:

$$I_p = 2.69 \times 10^5 n^{3/2} A D^{1/2} \nu^{1/2} C_p \quad (1)$$

where I_p is the peak current (A), n is the number of electrons transferred in the reaction, A is the active surface area (cm^2), D is the diffusion coefficient (7.6×10^{-6} cm^2 s^{-1} for 5.0 mM $[Fe(CN)_6]^{3-/4-}$ containing 0.1 M KCl), ν is the scan rates (V s^{-1}) and C_p is the concentration of the redox species (mol cm^{-3}). The electroactive surface area of bare GCE, AuNPs/GCE, AC/GCE and AuNPs/AC/GCE was found to be 0.0468, 0.1722, 0.1603 and 0.2630 cm^2, respectively.

Furthermore, the change of impedance of the modified electrode surface was proven by electrochemical impedance spectroscopy (EIS). The impedance data was obtained by fitting the Randles's circuit (Fig. 3B inset) which the semicircle parameters correspond to the charge transfer resistance (R_{ct}) and the diffusion impedance (Z_W) were both in parallel with the interface capacitance (C_{dl}). Figure 3B displays Nyquist plots of $[Fe(CN)_6]^{3-/4-}$ at bare GCE, AuNPs/GCE, AC/GCE and AuNPs/AC/GCE. The value of R_{ct} was found to be 110, 40, 22 and 15 Ω for bare GCE, AuNPs/GCE, AC/GCE and AuNPs/AC/GCE, respectively. The results indicated that the AuNPs/AC/GCE provided the lowest R_{ct} implying

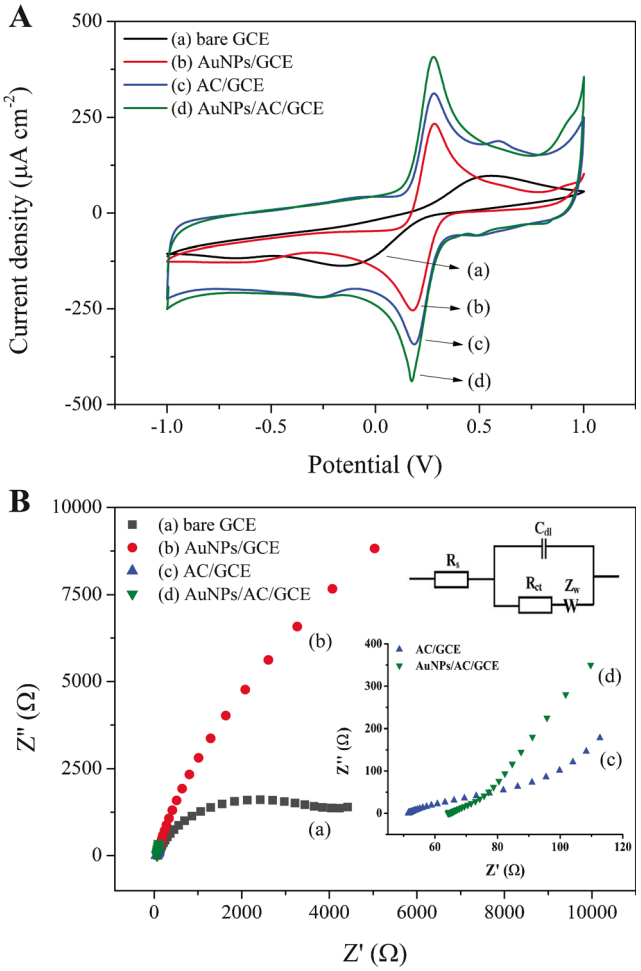

Fig. 3 (**A**) Cyclic voltammograms of 5 mM $[Fe(CN)_6]^{3-/4-}$ in 0.1 M KCl at bare GCE, AuNPs/GCE, AC/GCE and AuNPs/AC/GCE with scan rate of 50 mV s^{-1} and potential of −1.0 V to +1.0 V. (**B**) Nyquist plots of 5 mM $[Fe(CN)_6]^{3-/4-}$ in 0.1 M KCl at bare GCE, AuNPs/GCE, AC/GCE and AuNPs/AC/GCE, Inset: Nyquist plots at AC/GCE and AuNPs/AC/GCE with the frequency range of 0.001–100 kHz

the highest electroconductivity [27, 28]. Therefore, from all characterization results, the surface modification of GCE electrode with AuNPs and AC was successful.

Electrochemical behavior of CIP on AuNPs/AC/GCE

In this work, the electrochemical behavior of CIP on AuNPs/AC/GCE was studied by CV. It was found that the voltammogram of the phosphate buffer system (the black line in Fig. S7) exhibited an oxidation peak at 0.92 V and reduction peak at 0.59 V which were the peaks of AuNPs (Au(III) to Au(0)) [46, 47]. In the presence of CIP, the peak current of AuNPs was obviously decreased due to adsorption of CIP on the surface of electrode. The nitrogen atom of the CIP piperazine group could interact with AuNPs, thus decreasing the intensity of AuNPs [48, 49]. Therefore, in this study, the experimental results were evaluated using the change of AuNPs current (ΔI) under conditions with and without CIP. Although CIP affected both oxidation and reduction peaks of AuNPs, only the reduction peak (cathodic current) of AuNPs was employed because of its easier to interpret as displayed in Fig. S7.

The electrochemical reaction of CIP based on different pH solution was studied in the pH range from 4.0 to 8.0 using AuNPs/AC/GCE. CIP possesses positively charged at pH < 5.86, zwitterion at 5.86 < pH < 8.24, and negatively charged at pH > 8.24 [50, 51]. Figure 4A and S8 display the influence of pH on the peak current and ΔI of AuNPs in the presence of CIP, respectively. It was found that the peak intensity and ΔI were enhanced with the increasing of pH until pH 6.0 and thereafter significantly decreased. Moreover, the voltammograms showed that when pH decreased, the anodic and cathodic peak potentials of AuNPs were more positive potential suggesting the involvement of protons with oxidation of CIP. At pH 6.0, the zwitterion CIP was easily oxidized and the maximum peak current of AuNPs was achieved [50, 52]. According to Nernst equation [45], the relationship between E_p and pH is described as following equation:

$$E_p = \frac{0.0592m}{n} pH + b \quad (2)$$

where E_p is the peak potential (V), m and n are the number of protons and electrons in the electrochemical reaction, respectively, and b is the intercept of equation. The plot of peak potential (E_p) and pH (Fig. 4B) reveals that the linear relationship expressed as follows: $E_p = -0.0678pH + 1.0011$ ($r^2 = 0.9927$). It is clearly seen that the linear slope of 67.8 mV pH^{-1} is closed to the theoretical value 59.2 mV pH^{-1}, implying that the number of protons and electrons transferred in the reaction of CIP was equal [53].

In order to study the electrochemical mechanism, the effect of scan rate (ν) on the peak current and potential at AuNPs/AC/GCE was investigated using CV. The CVs of AuNPs (Fig. 5) in the presence of 0.5 μM CIP were recorded at different scan rates from 10 to 100 mV s^{-1}, which the potential shifted with increasing the scan rate, confirms the irreversible system. The relationship between ΔI and ν was linear with a regression equation of $\Delta I = 0.5607\nu + 5.0010$ ($r^2 = 0.9910$) as shown in Fig. S9, indicating an adsorption-controlled process [54]. In addition, a linear relation was obtained between potential and lnν (Fig. 5 inset): $E_p = -0.0211\ln\nu + 0.6771$ ($r^2 = 0.9961$). According to Laviron theory [55], the number of electrons involved in CIP oxidation for the irreversible reaction can be calculated following equation:

$$E_p(V) = E^o - \frac{RT}{\alpha nF} ln \frac{RTk_s}{\alpha nF} + \frac{RT}{\alpha nF} ln\nu \quad (3)$$

where E^o is the formal peak potential (V), α is the electron transfer coefficient, n is the number of electrons, F is the Faraday's constant (96,500 C mol^{-1}), R is the gas constant

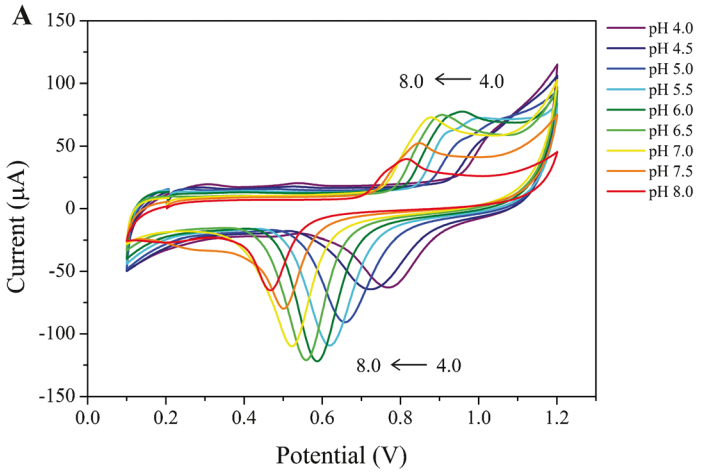

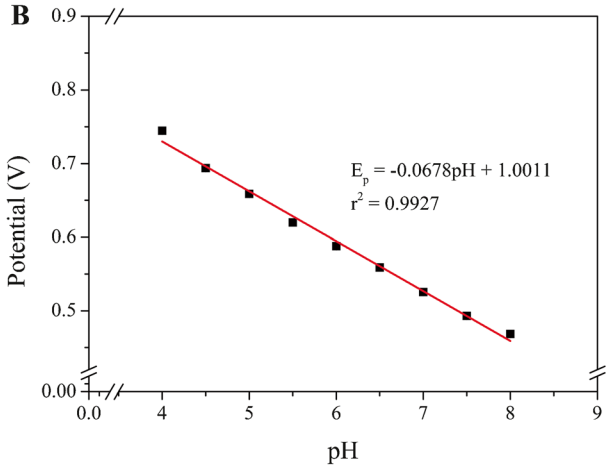

Fig. 4 (**A**) Cyclic voltammograms of AuNPs with 0.5 μM CIP in 0.1 M phosphate buffer at AuNPs/AC/GCE at various pH (4.0–8.0). The scan rate and potential were 50 mV s^{-1} and + 0.1 V to +1.2 V, respectively. (**B**) Linear relationship between the peak potential and pH of 0.5 μM CIP in 0.1 M phosphate buffer at AuNPs/AC/GCE

(8.314 J mol^{-1} K^{-1}), T is the temperature (298.15 K) and k_s is the standard heterogeneous reaction rate constant. From the slope of E_p versus lnν, the calculated value of αn of 1.22 was achieved which α was assumed to be 0.5 for the irreversible progress [19]. Therefore, the number of electrons in the CIP oxidation reaction was evaluated to be 2 being consistent with previous reports [16, 19]. The reaction of CIP at AuNPs/AC/GCE is demonstrated in Scheme S1.

Enhancement of sensitivity for CIP detection using SUPRAS

Surfactants have been reported that can improve electrochemical sensitivity by accelerating the diffusion of compounds toward the surface of electrode [32]. Moreover, they act as a stabilizer that assist AuNPs dispersion and result in the enhancement of the AuNPs signal [56]. This work used SUPRAS prepared from 5 mM DTAB and 2.5 mM DDAB in the presence of NaCl, to improve AuNPs signal and enrich CIP on the surface of electrode. The process for CIP detection at SUPRAS–AuNPs/AC/GCE is illustrated in Fig. S10. All the parameters in the SUPRAS system were optimized using DPV in the presence of 20 nM CIP in 0.1 M phosphate buffer at SUPRAS–AuNPs/AC/GCE. Figure S11 displays the DPV voltammograms of AuNPs in 0.1 M phosphate buffer without the addition of CIP. It was found that the peak current of AuNPs at SUPRAS–AuNPs/AC/GCE was higher than AuNPs/AC/GCE with a slightly negative shift of peak potential indicated SUPRAS can enhance the AuNPs signal.

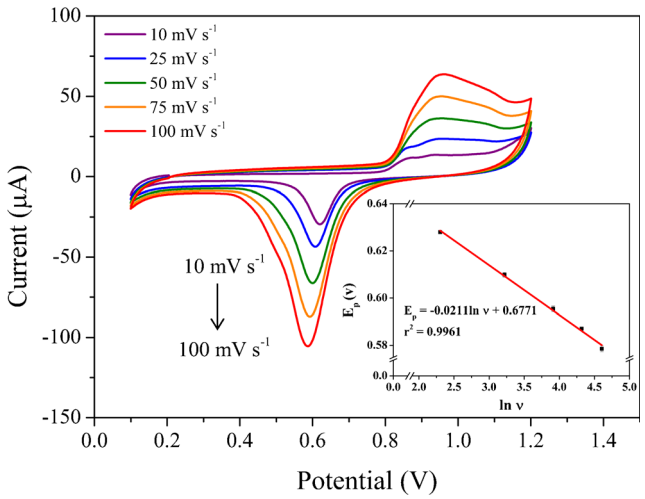

Fig. 5 Cyclic voltammograms of AuNPs in the presence of 0.5 μM CIP in 0.1 M phosphate buffer (pH 6.0) at different scan rates (10–100 mV s^{-1}) and potential of +0.1 V to +1.2 V at AuNPs/AC/GCE, Inset: linear relationship between the peak potential and natural logarithm of scan rate

Effect of types of surfactant

Two individual surfactants (5 mM DTAB and 2.5 mM DDAB) and SUPRAS were tested. The results (Fig. S12A) reveal that ΔI slightly increased ca. 1.7 times with the individual surfactants compared with phosphate buffer system (without surfactant). Meanwhile, the SUPRAS significantly enhanced the sensitivity of CIP which the ΔI was increased ca. 8.3 times, resulted from the increase of electron transfer rate [32, 33]. Hence, the SUPRAS was used throughout.

Furthermore, the concentrations of both surfactants were varied in the range of 1.2–7.4 mM (fixed molar ratio of DDAB:DTAB at 1:2 which is the optimum ratio to form SUPRAS [39]). It was found that (Fig. S12B) the ΔI increased with the increasing DDAB:DTAB concentration up to 2.5:5.0 mM and then it was decreased, this may be due to high concentration of SUPRAS covered the surface electrode. Therefore, the SUPRAS prepared from DDAB

and DTAB at 2.5 and 5.0 mM, respectively, was selected for further studies.

Effect of pH

The influence of pH was studied in the range of 4.0–11.0 at AuNPs/AC/GCE using 0.1 M phosphate buffer with the addition of SUPRAS. The results (Fig. S12C) showed that the ΔI increased until pH 10.0 and then sharply decreased. At pH < 8.24, CIP has the positive charge and zwitterion which interact poorly with the cationic SUPRAS. While at pH > 8.24, it is deprotonated; thus, the sensitivity of CIP was increased via electrostatic interaction between the anionic CIP and the cationic SUPRAS. Hence, pH 10.0 of phosphate buffer was chosen for further experiments.

The possible mechanism between CIP and SUPRAS was proved by zeta potential analysis. It was found that the prepared SUPRAS has a positive charge with the potential of 20 ± 2.08 mV (n = 3). After the addition of SUPRAS into CIP solution, the positive potential of 12 ± 0.76 mV (n = 3) of CIP–SUPRAS was observed. The result indicated that the decreasing of potential for CIP and SUPRAS system was obtained due to the negative charge of CIP interacted with the positive charged of SUPRAS via electrostatic attraction.

Analytical performance

The analytical performance of two fabricated sensors, namely AuNPs/AC/GCE and SUPRAS–AuNPs/AC/GCE, was evaluated using DPV under their optimal conditions. The analytical features studied are linearity, detection limit (LOD) and quantification limit (LOQ). Figure 6 displays the voltammograms of AuNPs at a potential range from +0.4 V to +0.9 V in the presence of different CIP concentrations using both electrochemical sensors. The current of AuNPs decreased with increasing CIP concentration from 0 to 1000 nM and 0 to 25 nM for AuNPs/AC/GCE and SUPRAS–AuNPs/AC/GCE, respectively. As summarized in Table 1, the linearity obtained from AuNPs/AC/GCE and SUPRAS–AuNPs/AC/GCE was ranged from 20 to 1000 nM and 0.5 to 25 nM with a determination coefficient (r^2) of 0.9935 and 0.9908, respectively. The LOD and LOQ were calculated according to the equations: LOD = 3σ/S and LOQ = 10σ/S, where σ is the standard deviation of blank (n = 7) and S is the slope of the calibration plot. The obtained LODs by AuNPs/AC/GCE and SUPRAS–AuNPs/AC/GCE were found to be 10 nM and 0.20 nM, and LOQs were 30 nM and 0.67 nM, respectively. The electrochemical sensitivity of 12.12 and 3962.64 μA μM^{-1} cm^{-2} for AuNPs/AC/GCE and SUPRAS–AuNPs/AC/GCE was achieved. The results indicated that SUPRAS–AuNPs/AC/GCE exhibited higher sensitivity for CIP detection than AuNPs/AC/GCE. In addition, the performance of SUPRAS–AuNPs/AC/GCE sensor was compared with the previous reports as summarized in Table 2. It can be seen that the linear range of the fabricated sensor was comparable to the others. This method was more sensitive than most of the reports which provided low LOD comparable to SSB–Apt/SPGE [57]; however, the proposed sensor (SUPRAS–AuNPs/AC/GCE) was simpler and more cost-effective than SSB–Apt/SPGE.

Interferences, reproducibility and stability

The effect of potential interferences from other antibiotics such as amoxicillin (AMX), tetracycline (TC), oxytetracycline (OTC), enrofloxacin (ENR), ofloxacin (OFL) and norfloxacin

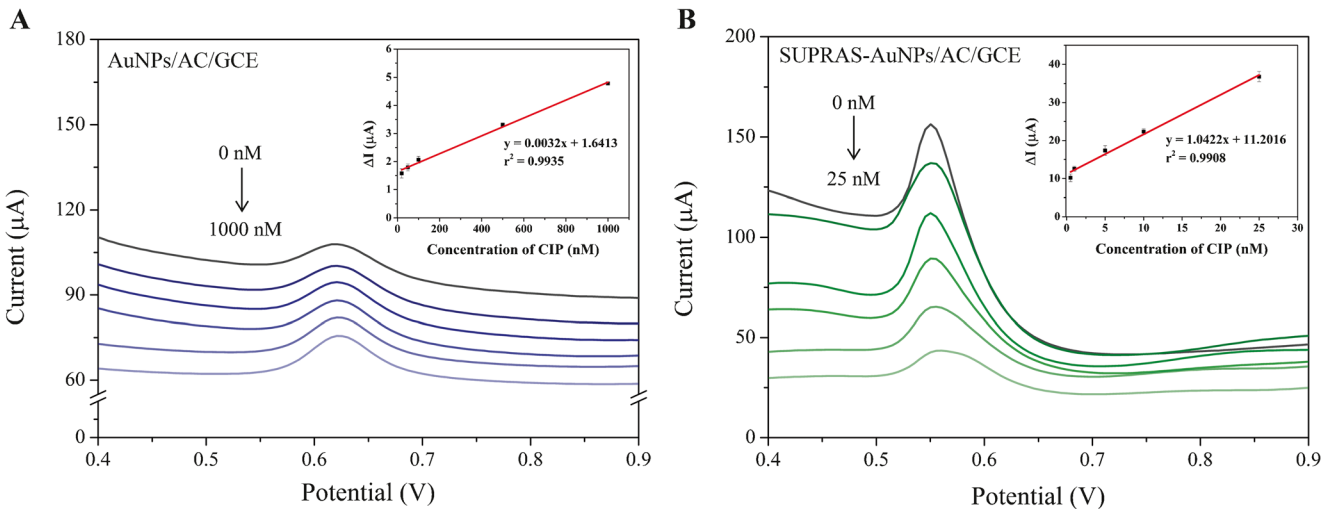

Fig. 6 Differential pulse voltammograms of AuNPs in the presence of different concentration of CIP in 0.1 M phosphate buffer (**A**) pH 6.0 at AuNPs/AC/GCE and (**B**) pH 10.0 at SUPRAS–AuNPs/AC/GCE, Inset: calibration plot of AuNPs/AC/GCE and SUPRAS–AuNPs/AC/GCE sensors obtained from DPV measurement with potential of +1.2 to +0.2 V

Table 1 Analytical parameters of the fabricated electrochemical sensors

Parameter	Fabricated electrochemical sensor	
	AuNPs/AC/GCE	SUPRAS–AuNPs/AC/GCE
Linear equation	y=0.0032x+1.6413	y=1.0422x+11.2016
r^2	0.9935	0.9908
Linear range (nM)	20–1000	0.5–25
LOD (nM)	10	0.20
LOQ (nM)	30	0.67
Sensitivity ($\mu A\ \mu M^{-1}\ cm^{-2}$)	12.12	3962.64
%RSD intra-day (n=5)*	1.3%	3.8%
%RSD inter-day (n=5×3)*	2.6%	8.6%

*CIP 100 nM for AuNPs/AC/GCE and CIP 1 nM for SUPRAS–AuNPs/AC/GCE

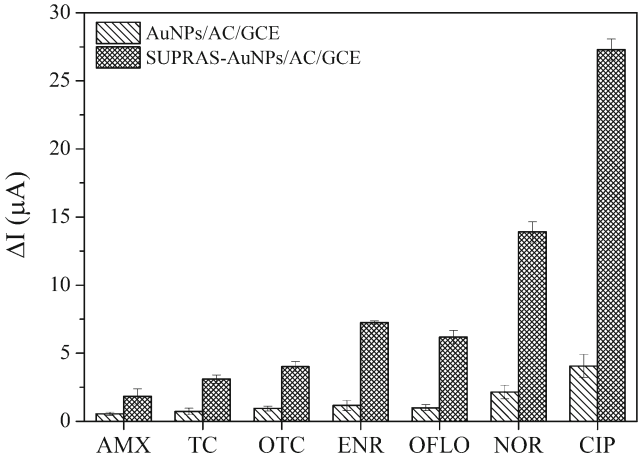

Fig. 7 Selectivity of AuNPs/AC/GCE and SUPRAS–AuNPs/AC/GCE with various antibiotics (20 nM of each) in 0.1 M phosphate buffer (pH 6.0 for AuNPs/AC/GCE and pH 10.0 for SUPRAS–AuNPs/AC/GCE)

(NOR) was studied by DPV using AuNPs/AC/GCE and SUPRAS–AuNPs/AC/GCE. The concentration of all tested antibiotics was 20 nM. As can be seen in Fig. 7, AMX, TC and OTC did not significantly affect to AuNPs signal. While ENR, OFL, and NOR had an effect on the DPV signal, may due to these compounds are in the same group with CIP, especially NOR having piperazine group in its structure. However, CIP gave the highest sensitivity under the studied conditions for the fabricated electrochemical sensor.

The reproducibility of the AuNPs/AC/GCE and SUPRAS–AuNPs/AC/GCE sensors was investigated by DPV detection of 100 nM CIP in 0.1 M phosphate buffer (pH 6.0) and 1 nM CIP in 0.1 M phosphate buffer (pH 10.0), respectively. Under the optimized conditions, the precision of two fabricated sensors, in terms of relative standard deviation (RSD, $n = 5$), was found to be less than 3.8% and 8.6% in a day (intra-day) and 3

Table 2 Comparison of the proposed sensor (SUPRAS–AuNPs/AC/GCE) with other sensors for CIP detection

Modified electrode	Linear range (μM)	LOD (nM)	Sensitivity ($\mu A\ \mu M^{-1}\ cm^{-2}$)	Sample	Detection technique	Reference
NiONPs–GO–CTS:EPH/GCE	0.040–0.97	6.0	29.91	Serum, urine	SWV	[15]
rGO/PPR/GCE	0.002–0.05, 0.05–400	2	516.41, 0.239	Serum	DPV	[16]
TiO_2/PB/AuNPs/CMK–3/Nafion/GE	1–10	108	56.89	Water	CV	[17]
O–BDDP–printed electrode	1–30	588	0.215	Urine	LSV	[18]
AuNPs/CHI/SPE	0.1–150	1	0.016	Serum, plasma, urine	SWV	[19]
CNT–V_2O_5–CS/SPE	1.5–24*	1.5	–	Milk	EIS	[21]
PEI@Fe_3O_4@CNTs/GCE	0.03–5, 5–70	3.0	73.39, 7.89	Serum, urine, pharmaceutical	DPV	[22]
SSB–Apt/SPGE	0.8–400*	0.26	–	Serum, milk, water	DPV	[57]
SUPRAS–AuNPs/AC/GCE	0.5–25*	0.20	3962.64	Milk, pharmaceutical	DPV	This work

*Linear range in nM unit

NiONPs–GO–CTS:EPH/GCE; nickel oxide nanoparticles–graphene oxide–chitosan: epichlorohydrin on GCE

rGO/PPR/GCE; reduced graphene oxide/poly(phenol red) on GCE

TiO_2/PB/AuNPs/CMK–3/Nafion/GE; titanium dioxide sol, AuNPs, CMK–3 type mesoporous carbon and Nafion nanocomposite on GE

O–BDDP–printed electrode; oxygen-terminated boron–doped diamond–printed electrode

AuNPs/CHI/SPE; AuNPs/chitosan polymer on SPE

CNT–V_2O_5–CS/SPE; carbon nanotube–V_2O_5–chitosan nanocomposites on SPE

PEI@Fe_3O_4@CNTs/GCE; polyethylenimine@Fe_3O_4@carbon nanotube nanocomposite on GCE

SSB–Apt/SPGE; single-stranded DNA–binding protein/aptamer on screen-printed gold electrodes

Table 3 Recovery studies of spiked CIP in milk samples ($n = 3$)

Spiked (nM)	Raw milk			UHT milk			0% fat milk		
	Found ± SD (nM)	%Recovery± SD	%RSD	Found ± SD (nM)	%Recovery± SD	%RSD	Found ± SD (nM)	%Recovery± SD	%RSD
0.5	0.47 ± 0.04	93.2 ± 7.47	8.0	0.55 ± 0.05	110.2 ± 9.22	8.4	0.43 ± 0.03	86.8 ± 5.49	6.3
5	5.25 ± 0.33	105.0 ± 6.70	6.4	4.77 ± 0.36	95.3 ± 7.19	7.5	4.56 ± 0.28	91.1 ± 5.65	6.2
20	18.46 ± 1.15	92.3 ± 5.77	6.2	17.28 ± 1.30	86.4 ± 6.48	7.5	15.72 ± 0.93	78.6 ± 4.64	5.9
HPLC analysis at 20 nM	18.55 ± 0.35	92.8 ± 1.75	1.9	17.93 ± 0.61	89.6 ± 3.03	3.4	15.98 ± 0.74	79.9 ± 3.71	4.6

consecutive days (inter-day), respectively, as summarized in Table 1. Furthermore, the stability of the sensors was also evaluated at 20 nM CIP using one electrode. The results (Fig. S13) indicated that the signals in terms of percent relative were decreased and the signal in terms of ΔI increased ca. 10% after 13 cycles and 6 cycles usage of AuNPs/AC/GCE and SUPRAS–AuNPs/AC/GCE, respectively. It can be concluded that the fabricated sensors had not only good selectivity but also good reproducibility and stability for the detection of CIP.

Sample analysis

The applicability of the SUPRAS–AuNPs/AC/GCE sensor was examined for the detection of CIP in milk samples including raw milk, UHT milk and 0% fat milk. In this study, to reduce the using of organic solvents, SUPRAS was used instead to deproteinize and defat of milk sample. Milk proteins, such as casein and lactoglobulin, and fat were removed through electrostatic interaction between the ionic head group of surfactant and ionic groups of milk proteins, and hydrophobic interaction between alkyl chains of surfactant and hydrophobic part of milk proteins [58, 59]. All milk samples were spiked with three concentration levels of CIP (0.5, 5 and 20 nM) and the detection was performed in triplicate. The recovery of CIP was achieved in the range of 78.6–110.2% with RSDs less than 8.4% as shown in Table 3. The results from the fabricated sensor at 20 nM CIP were compared with HPLC which they are in good agreement. Moreover, the proposed sensor was used to determine CIP in pharmaceutical formulations. Two tablet samples were dissolved and diluted in water at an appropriate volume ratio. It was found that the obtained CIP amount was 496.04 and 492.82 mg (Table 4) which close to a labeled value (500 mg/tablet), indicating that the fabricated sensor (SUPRAS–AuNPs/AC/GCE) is effective and accurate for the determination of CIP in real samples.

Table 4 The determination of CIP in pharmaceutical formulations (n = 3)

Sample	Labeled value (mg/tablet)	Found±SD (mg/tablet)	%Relative accuracy±SD	%RSD
Tablet 1	500	496.04 ± 13.57	99.2 ± 2.71	2.7
Tablet 2	500	492.82 ± 15.05	98.6 ± 3.01	3.1

Conclusion

A novel and sensitive electrochemical sensor using GCE modified with AC and AuNPs in the presence of SUPRAS (SUPRAS–AuNPs/AC/GCE) was fabricated to determine CIP. The sensitivity of the electrochemical sensor was attributed to greatly increased electroactive area and conductivity resulting from AC and AuNPs. Moreover, the sensitivity was further increased through SUPRAS, which facilitating electron transfer of AuNPs and enrich CIP on the electrode surface. Besides the ease and low-cost fabrication, this proposed innovative sensor can be considered as eco-friendly sensor from the usage of green solvent (SUPRAS) and the recycle of biomass waste (waste coffee ground) for AC precursor. The proposed method is interfered by NOR at high concentration. SUPRAS–AuNPs/AC/GCE was successfully applied for the detection of CIP in milk and pharmaceutical samples.

Supplementary Information The online version contains supplementary material available at https://doi.org/10.1007/s00604-021-04869-z.

Author contribution Netsirin Gissawong: Conceptualization, methodology, investigation, writing—original draft. Supalax Srijaranai: Supervision, writing—review and editing. Suthasinee Boonchiangma: Investigation, visualization. Pikaned Uppachai: Methodology, validation, visualization. Kompichit Seehamart: Methodology. Sakwiboon Jantrasee: Methodology. Eric Moore: Writing—review and editing. Siriboon Mukdasai: Conceptualization, supervision, writing—review and editing.

Funding The financial support from the Science Achievement Scholarship of Thailand (SAST) for N. Gissawong is gratefully acknowledged. Financial support from Materials Chemistry Research Center (MCRC) and the Center of Excellence for Innovation in Chemistry (PERCH–CIC), Ministry of Higher Education, Science, Research and Innovative, Thailand, are also gratefully acknowledged.

Compliance with ethical standards

Conflict of interest The authors declare no competing interests.

References

1. Yan H, Row KH, Yang G (2008) Water–compatible molecularly imprinted polymers for selective extraction of ciprofloxacin from human urine. Talanta 75(1):227–232. https://doi.org/10.1016/j.talanta.2007.11.002
2. Tiwari M, Kumar A, Shankar U, Prakash R (2016) The nanocrystalline coordination polymer of AMT–Ag for an effective detection of ciprofloxacin hydrochloride in pharmaceutical formulation and biological fluid. Biosens Bioelectron 85:529–535. https://doi.org/10.1016/j.bios.2016.05.049
3. Surya SG, Khatoon S, Lahcen AA, Nguyen ATH, Dzantiev BB, Tarannum N, Salama KN (2020) A chitosan gold nanoparticles molecularly imprinted polymer based ciprofloxacin sensor. RSC Adv 10:12823–12832. https://doi.org/10.1039/D0RA01838D
4. Moghadam NR, Arefhosseini SR, Javadi A, Lotfipur F, Ansarin M, Tamizi E, Nemati M (2018) Determination of enrofloxacin and ciprofloxacin residues in five different kinds of chicken tissues by dispersive liquid–liquid microextraction coupled with HPLC. Iran J Pharm Res 17(4):1182–1190
5. Hoof NV, Wasch KD, Okerman L, Reybroeck W, Poelmans S, Noppe H, Brabander HD (2005) Validation of a liquid chromatography–tandem mass spectrometric method for the quantification of eight quinolones in bovine muscle, milk and aquacultured products. Anal Chim Acta 529(1–2):265–272. https://doi.org/10.1016/j.aca.2004.07.055
6. Okerman L, Noppe H, Cornet V, Zutter LD (2007) Microbiological detection of 10 quinolone antibiotic residues and its application to artificially contaminated poultry samples. Food Addit Contam 24(3):252–257. https://doi.org/10.1080/02652030600988020
7. Hashemi SH, Ziyaadini M, Kaykhaii M, Keikha AJ, Naruie N (2020) Separation and determination of ciprofloxacin in seawater, human blood plasma and tablet samples using molecularly imprinted polymer pipette–tip solid phase extraction and its optimization by response surface methodology. J Sep Sci 43(2):505–513. https://doi.org/10.1002/jssc.201900923
8. Taghizade M, Ebrahimi M, Fooladi E, Yoosefian M (2021) Simultaneous spectrophotometric determination of the residual of ciprofloxacin, famotidine, and tramadol using magnetic solid phase extraction coupled with multivariate calibration methods. Microchem J 160:105627. https://doi.org/10.1016/j.microc.2020.105627
9. Li Z, Cui Z, Tang Y, Liu X, Zhang X, Liu B, Wang X, Draz MS, Gao X (2019) Fluorometric determination of ciprofloxacin using molecularly imprinted polymer and polystyrene microparticles doped with europium(III)$(DBM)_3$phen. Microchim Acta 186:334. https://doi.org/10.1007/s00604-019-3448-z
10. Wang B, Yan B (2020) A turn–on fluorescence probe Eu^{3+} functionalized Ga–MOF integrated with logic gate operation for detecting ppm–level ciprofloxacin (CIP) in urine. Talanta 208:120438. https://doi.org/10.1016/j.talanta.2019.120438
11. Szerkus O, Jacyna J, Gibas A, Sieczkowski M, Siluk D, Matuszewski M, Kaliszan R, Markuszewski MJ (2017) Robust HPLC–MS/MS method for levofloxacin and ciprofloxacin determination in human prostate tissue. J Pharm Biomed 132:173–183. https://doi.org/10.1016/j.jpba.2016.10.008
12. Ferrone V, Carlucci M, Cotellese R, Raimondi P, Cichella A, Marco LD, Carlucci G (2017) Development and validation of a fast microextraction by packed sorbent UHPLC–PDA method for the simultaneous determination of linezolid and ciprofloxacin in human plasma from patients with hospital–acquired pneumonia. Talanta 164:64–68. https://doi.org/10.1016/j.talanta.2016.11.014
13. Rassaei L, Amiri M, Cirtiu CM, Sillanpää M, Marken F, Sillanpää M (2011) Nanoparticles in electrochemical sensors for environmental monitoring. Trends Anal Chem 30(11):1704–1715. https://doi.org/10.1016/j.trac.2011.05.009
14. Power AC, Gorey B, Chandra S, Chapman J (2018) Carbon nanomaterials and their application to electrochemical sensors: a review. Nanotechnol Rev 7(1):19–41. https://doi.org/10.1515/ntrev-2017-0160
15. Santos AM, Wong A, Almeida AA, Fatibello–Filho O (2017) Simultaneous determination of paracetamol and ciprofloxacin in biological fluid samples using a glassy carbon electrode modified with oxide of graphene and nickel oxide nanoparticles. Talanta 174:610–618. https://doi.org/10.1016/j.talanta.2017.06.040
16. Chauhan R, Gill AAS, Nate Z, Karpoormath R (2020) Highly selective electrochemical detection of ciprofloxacin using reduced graphene oxide/poly(phenol red) modified glassy carbon electrode. J Electroanal Chem 871:114254. https://doi.org/10.1016/j.jelechem.2020.114254
17. Pollap A, Baran K, Kuszewska N, Kochana J (2020) Electrochemical sensing of ciprofloxacin and paracetamol in environmental water using titanium sol based sensor. J Electroanal Chem 878:114574. https://doi.org/10.1016/j.jelechem.2020.114574
18. Matsunaga T, Kondo T, Osasa T, Kotsugai A, Shitanda I, Hoshi Y, Itagaki M, Aikawa T, Tojo T, Yuasa M (2020) Sensitive electrochemical detection of ciprofloxacin at screen–printed diamond electrodes. Carbon 159:247–254. https://doi.org/10.1016/j.carbon.2019.12.051
19. Reddy KR, Brahman PK, Suresh L (2018) Fabrication of high performance disposable screen printed electrochemical sensor for ciprofloxacin sensing in biological samples. Measurement 127:175–186. https://doi.org/10.1016/j.measurement.2018.05.078
20. Mukdasai S, Poosittisak S, Ngeontae W, Srijaranai S (2018) A highly sensitive electrochemical determination of L–tryptophan in the presence of ascorbic acid and uric acid using in situ addition of tetrabutylammonium bromide on the β–cyclodextrin incorporated multiwalled carbon nanotubes modified electrode. Sensors Actuators B Chem 272:518–525. https://doi.org/10.1016/j.snb.2018.06.014
21. Hu X, Goud KY, Kumar VS, Catanante G, Li Z, Zhu Z, Marty JL (2018) Disposable electrochemical aptasensor based on carbon nanotubes–V_2O_5–chitosan nanocomposite for detection of ciprofloxacin. Sensors Actuators B Chem 268:278–286. https://doi.org/10.1016/j.snb.2018.03.155
22. Jalal NR, Madrakian T, Afkhami A, Ghamsari M (2019) Polyethylenimine@Fe_3O_4@carbon nanotubes nanocomposite as a modifier in glassy carbon electrode for sensitive determination of ciprofloxacin in biological samples. J Electroanal Chem 833:281–289. https://doi.org/10.1016/j.jelechem.2018.12.004
23. Madhu R, Veeramani V, Chen SM (2014) Fabrication of a novel gold nanospheres/activated carbonnanocomposite for enhanced electrocatalytic activity toward the detection of toxic hydrazine in various water samples. Sensors Actuators B Chem 204:382–387. https://doi.org/10.1016/j.snb.2014.07.068
24. Ni Y, Xu J, Liang Q, Shao S (2017) Enzyme–free glucose sensor based on heteroatom–enriched activatedcarbon (HAC) decorated with hedgehog–like NiO nanostructures. Sensors Actuators B Chem 250:491–498. https://doi.org/10.1016/j.snb.2017.05.004
25. Dubey P, Shrivastav V, Maheshwari PH, Sundriyal S (2020) Recent advances in biomass derived activated carbon electrodes for hybrid electrochemical capacitor applications: challenges and opportunities. Carbon 170:1–29. https://doi.org/10.1016/j.carbon.2020.07.056

26. Guo S, Wang E (2007) Synthesis and electrochemical applications of gold nanoparticles. Anal Chim Acta 598(2):181–192. https://doi.org/10.1016/j.aca.2007.07.054
27. Kumar N, Rosy GRN (2017) Gold–palladium nanoparticles aided electrochemically reduced graphene oxide sensor for the simultaneous estimation oflomefloxacin and amoxicillin. Sensors Actuators B Chem 243:658–668. https://doi.org/10.1016/j.snb.2016.12.025
28. Liu Z, Jin M, Cao J, Wang J, Wang X, Zhou G, Berg A, Shui L (2018) High–sensitive electrochemical sensor for determination of norfloxacin and its metabolism using MWCNT–CPE/pRGO–ANSA/Au. Sensors Actuators B Chem 257:1065–1075. https://doi.org/10.1016/j.snb.2017.11.052
29. Wong A, Santos AM, Fatibello–Filho O (2018) Simultaneous determination of paracetamol and levofloxacin using a glassy carbon electrode modified with carbon black, silvernanoparticles and PEDOT:PSS film. Sensors Actuators B Chem 255:2264–2273. https://doi.org/10.1016/j.snb.2017.09.020
30. Ghanbari MH, Khoshroo A, Sobati H, Ganjali MR, Rahimi–Nasrabadi M, Ahmadi F (2019) An electrochemical sensor based on poly (L–cysteine)@AuNPs@reduced graphene oxide nanocomposite for determination of levofloxacin. Microchem J 147:198–206. https://doi.org/10.1016/j.microc.2019.03.016
31. Zhu M, Li R, Lai M, Ye H, Long N, Ye J, Wang J (2020) Copper nanoparticles incorporating a cationic surfactant–graphene modified carbon paste electrode for the simultaneous determination of gatifloxacin and pefloxacin. J Electroanal Chem 857:113730. https://doi.org/10.1016/j.jelechem.2019.113730
32. Vittal R, Gomathi H, Kim KJ (2006) Beneficial role of surfactants in electrochemistry and in the modification of electrodes. Adv Colloid Interf Sci 119(1):55–68. https://doi.org/10.1016/j.cis.2005.09.004
33. Fekry AM, Azab SM, Shehata M, Ameer MA (2015) A novel electrochemical nicotine sensor based on cerium nanoparticles with anionic surfactant. RSC Adv 5:51662–51671. https://doi.org/10.1039/C5RA06024A
34. Shehata M, Azab SM, Fekry AM, Ameer MA (2016) Nano–TiO_2 modified carbon paste sensor for electrochemical nicotine detection using an ionic surfactant. Biosens Bioelectron 79:589–592. https://doi.org/10.1016/j.bios.2015.12.090
35. Rubio S (2020) Twenty years of supramolecular solvents in sample preparation for chromatography: achievements and challenges ahead. Anal Bioanal Chem 412:6037–6058. https://doi.org/10.1007/s00216-020-02559-y
36. Ballesteros–Gómez A, Sicilia MD, Rubio S (2010) Supramolecular solvents in the extraction of organic compounds. A review Anal Chim Acta 677(2):108–130. https://doi.org/10.1016/j.aca.2010.07.027
37. Uppachai P, Srijaranai S, Poosittisak S, Isa IM, Mukdasai S (2020) Supramolecular electrochemical sensor for dopamine detection based on self–assembled mixed surfactants on gold nanoparticles deposited graphene oxide. Molecules 25(11):2528–2542. https://doi.org/10.3390/molecules25112528
38. Li G, Li J, Tan W, Jin H, Yang H, Peng J, Barrow CJ, Yang M, Wang H, Yang W (2016) Preparation and characterization of the hydrogen storage activated carbon from coffee shell by microwave irradiation and KOH activation. Int Biodeterior Biodegradation 113:386–390. https://doi.org/10.1016/j.ibiod.2016.05.003
39. Gissawong N, Boonchiangma S, Mukdasai S, Srijaranai S (2019) Vesicular supramolecular solvent–based microextraction followed by high performance liquid chromatographic analysis of tetracyclines. Talanta 200:203–211. https://doi.org/10.1016/j.talanta.2019.03.049
40. George JM, Antony A, Mathew B (2018) Metal oxide nanoparticles in electrochemical sensing and biosensing: a review. Microchim Acta 185:358–384. https://doi.org/10.1007/s00604-018-2894-3
41. Puziy AM, Poddubnaya OI, Socha RP, Gurgul J, Wisniewski M (2008) XPS and NMR studies of phosphoric acid activated carbons. Carbon 46(15):2113–2123. https://doi.org/10.1016/j.carbon.2008.09.010
42. Soliman AM, Elsuccary SAA, Ali IM, Ayesh AI (2017) Photocatalytic activity of transition metal ions–loaded activated carbon: degradation of crystal violet dye under solar radiation. J Water Process Eng 17:245–255. https://doi.org/10.1016/j.jwpe.2017.04.010
43. Wang Y, Yang P, Zheng L, Shi X, Zheng H (2020) Carbon nanomaterials with sp^2 or/and sp hybridization in energy conversion and storage applications: a review. Energy Storage Mater 26:349–370. https://doi.org/10.1016/j.ensm.2019.11.006
44. Jiang Z, Li G, Zhang M (2016) Electrochemical sensor based on electro–polymerization of β–cyclodextrin and reduced–graphene oxide on glassy carbon electrode for determination of gatifloxacin. Sensors Actuators B Chem 228:59–65. https://doi.org/10.1016/j.snb.2016.01.013
45. Bard AJ, Faulkner LR (2000) Electrochemical methods: fundamentals and applications, 2nd edn. Wiley, Hoboken, NJ, USA
46. Dudin PV, Unwin PR, Macpherson JV (2010) Electrochemical nucleation and growth of gold nanoparticles on single–walled carbon nanotubes: new mechanistic insights. J Phys Chem C 114(31):13241–13248. https://doi.org/10.1021/jp1043706
47. Hezard T, Fajerwerg K, Evrard D, Collière V, Behra P, Gros P (2012) Influence of the gold nanoparticles electrodeposition method on Hg(II) trace electrochemical detection. Electrochim Acta 73:15–22. https://doi.org/10.1016/j.electacta.2011.10.101
48. Tom RT, Suryanarayanan V, Reddy PG, Baskaran S, Pradeep T (2004) Ciprofloxacin–protected gold nanoparticles. Langmuir 20(5):1909–1914. https://doi.org/10.1021/la0358567
49. Nisar M, Khan SA, Qayum M, Khan A, Farooq U, Jaafar HZE, Zia–Ul–Haq M, Ali R (2016) Robust synthesis of ciprofloxacin–capped metallic nanoparticles and their urease inhibitory assay. Molecules 21(4):411–423. https://doi.org/10.3390/molecules21040411
50. Antilén M, Valencia C, Peralta E, Canales C, Espinosa–Bustos C, Escudey M (2017) Enrofloxacin behavior in presence of soil extracted organic matter: an electrochemical approach. Electrochim Acta 244:104–111. https://doi.org/10.1016/j.electacta.2017.05.104
51. Yang L, Qin X, Jiang X, Gong M, Yin D, Zhang Y, Zhao B (2015) SERS investigation of ciprofloxacin drug molecules on TiO_2 nanoparticles. Phys Chem Chem Phys 17:17809–17815. https://doi.org/10.1039/C5CP02666K
52. Shahrokhian S, Rastgar S (2012) Electrochemical deposition of gold nanoparticles on carbon nanotube coated glassy carbon electrode for the improved sensing of tinidazole. Electrochim Acta 78:422–429. https://doi.org/10.1016/j.electacta.2012.06.035
53. Bagheri H, Khoshsafar H, Amidi S, Ardakani YH (2016) Fabrication of an electrochemical sensor based on magnetic multiwalled carbon nanotubes for the determination of ciprofloxacin. Anal Methods 8:3383–3390. https://doi.org/10.1039/C5AY03410H
54. MA E, R, Wassel AA, NTA G, MA E, S (2005) Electrochemical adsorptive behaviour of some fluoroquinolones at carbon paste electrode. Anal Sci 21(10):1249–1254. https://doi.org/10.2116/analsci.21.1249
55. Laviron E (1979) General expression of the linear potential sweep voltammogram in the case of diffusionless electrochemical systems. J Electroanal Chem 101(1):19–28. https://doi.org/10.1016/S0022-0728(79)80075-3
56. Ma H, Yin B, Wang S, Jiao Y, Pan W, Huang S, Chen S, Meng F (2004) Synthesis of silver and gold nanoparticles by a novel electrochemical method. Chem Phys Chem 5(1):68–75. https://doi.org/10.1002/cphc.200300900

57. Abnous K, Danesh NM, Alibolandi M, Ramezani M, Taghdisi SM, Emrani AS (2017) A novel electrochemical aptasensor for ultrasensitive detection of fluoroquinolones based on single–stranded DNA–binding protein. Sensors Actuators B Chem 240:100–106. https://doi.org/10.1016/j.snb.2016.08.100
58. Ward K, Cheng SI, Stuckey DC (2016) Protein separation using non–ionic and cationic surfactant precipitation. J Chem Technol Biotechnol 91(10):2563–2567. https://doi.org/10.1002/jctb.4942
59. Wong FWF, Ariff AB, Stuckey DC (2018) Downstream protein separation by surfactant precipitation: a review. Crit Rev Biotechnol 38(1):31–46. https://doi.org/10.1080/07388551.2017.1312266